

Structure-preserving Optimal Kron-based Reduction of Radial Distribution Networks

Omid Mokhtari, *Member, IEEE*, Samuel Chevalier, *Member, IEEE*, and Mads Almassalkhi, *Senior Member, IEEE*

Abstract—Network reduction simplifies complex electrical networks to address computational challenges of large-scale transmission and distribution grids. Traditional network reduction methods are often based on a predefined set of nodes or lines to remain in the reduced network. This paper builds upon previous work on Optimal Kron-based Reduction of Networks (Opti-KRON), which was formulated as a mixed-integer linear program (MILP), to enhance the framework in two aspects. First, the scalability is improved via a cutting plane restriction, tightened Big M bounds, and a zero-injection node reduction stage. Next, we introduce a radiality-preservation step to identify and recover nodes whose restoration ensures radiality of the reduced network. The model is validated through its application to the 533-bus distribution test system and a 3499-bus realistic test feeder for a set of representative loading scenarios. In the 533-bus system, an 85% reduction was achieved with a maximum voltage error below 0.0025 p.u., while in the 3499-bus feeder, over 94% reduction was obtained with maximum voltage errors below 0.002 p.u. Additionally, we show that the radialization step accelerates the runtime of optimal voltage control problems when applied to Kron-reduced networks.

Index Terms—Optimal network reduction, radialization, Kron reduction, MILP, radial networks.

I. INTRODUCTION

MODERN power grids span large geographic areas and are becoming more complex due to integration of renewable energy resources and control devices, e.g., inverters [1]. Network reduction techniques are designed to mitigate this complexity by simplifying large networks while preserving essential system characteristics. Unfortunately, key operational characteristics, such as line flows and nodal voltages, are prone to inaccuracies in reduced networks relative to the original networks. Consequently, network reduction involves a trade-off between accuracy and the level of reduction, and the choice of an appropriate reduction technique depends on the relative importance of these metrics.

One method for network reduction is bus aggregation. This approach clusters buses that share similar characteristics, such as buses with similar power transfer distribution factors (PTDFs), which indicate that injections at these buses have similar effects on branch flows [2]–[4]. However, methods based on PTDFs neglect voltage deviations and have limited applicability in distribution feeders.

This material is based upon work supported by the U.S. Department of Energy’s Office of Energy Efficiency and Renewable Energy (EERE) under the Enabling Place-Based Renewable Power Generation using Community Energized Design initiative, award number DE-EE0010407. The views expressed herein do not necessarily represent the views of the U.S. Department of Energy or the United States Government.

O. Mokhtari, S. Chevalier, and M. Almassalkhi are with the Department of Electrical and Biomedical Engineering, University of Vermont, Burlington, VT 05405, USA {omid.mokhtari, schevali, malmassa}@uvm.edu.

Another network reduction approach is bus elimination, which is based on methods such as Ward [5] or Kron reduction [6]. This approach includes selecting a set of nodes to keep in the reduced network. For example, [7] partitions networks and separates important bus pairs into different clusters, then applies Kron reduction to reduce non-border buses within clusters. However, the reduction here is prioritized based on nodal degree and not based on an error metric, which might degrade the accuracy of the reduced model.

In addition to aggregation and elimination techniques, a range of data-driven, machine learning, and optimization-based approaches have been proposed for network reduction. Data-driven methods typically construct reduced models by fitting network parameters to match full-system responses across representative scenarios [8]–[10]. Similarly, optimization-based approaches usually aim to preserve specific characteristics, such as PTDF or impedance behaviors [11], [12]. However, such methods rely on a predetermined set of nodes or lines and lack the explicit ability to manage the balance between network complexity and voltage accuracy.

An Inversion Reduction method is proposed in [13] and [14] for distribution networks reduction. In both works, the user must predefine a set of salient buses to retain in the grid, and voltage accuracy is evaluated after the reduction rather than enforced during the process. As a result, the method cannot manage trade-offs between network size and voltage accuracy.

While existing methods often rely on predefined sets of nodes or lines to remain in the grid, the problem of identifying the set of nodes that optimally balances reduction level and model accuracy was initially been addressed in [15] with the Opti-KRON formulation. It formulates the optimal network reduction problem as an MILP, where integer variables indicate whether to remove or retain each node. While test cases in [15] were limited to 300 nodes, realistic networks usually span thousands of nodes. Also, the approach is based on Kron reduction, which can transform radial networks into dense, meshed networks [6]. This paper extends [15] by improving scalability and ensuring that the reduced distribution feeder preserves radiality through a new process termed *radialization*. Maintaining radiality enables the direct application of algorithms developed for radial distribution systems [16], [17] and supports convex conic formulations of power-flow problems [18]. Furthermore, the inherent sparsity of radial networks enhances the computational tractability of optimization and other power system analysis problems. Thus, radialization is regarded as important when Kron reduction is employed. An overview of the proposed optimal network reduction framework, including radialization, is illustrated in Fig. 1. This paper makes the following key contributions to the field of (optimal)

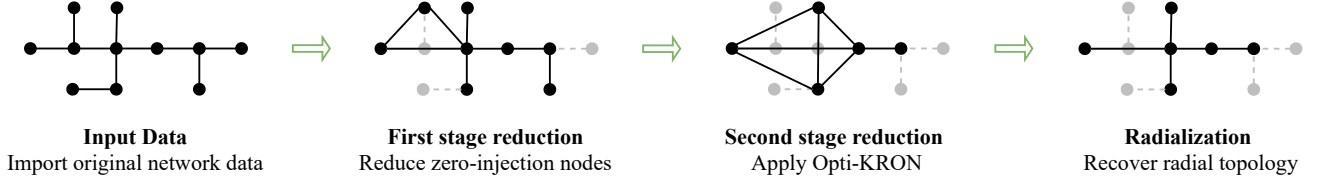


Fig. 1. Flow of the proposed network reduction framework. The first stage reduces the network by removing buses with no active elements (e.g., load or generation). The second stage iteratively applies the proposed optimization problem, i.e., Opti-KRON, to the initial reduced network until further reduction would violate voltage deviation limits. Finally, if the reduced network is meshed, radiality is restored by reintroducing a minimal set of previously reduced nodes. Radialization may also be applied after the first-stage reduction.

network reduction:

- **Scalability:** A two-stage reduction strategy is developed to extend Opti-KRON to realistic size networks. The first stage eliminates zero-injection nodes. In the second stage, the previously reduced network is further reduced through Opti-KRON, which is solved using a new cutting-plane method, tightly bounded Big M constraints, and a linear voltage-deviation constraint as a stopping criterion.
- **Radialization:** A novel method is proposed to find an equivalent radial network from a Kron reduced network by identifying and reinserting a minimal set of previously reduced nodes.
- **Simulation-based analysis:** The proposed framework is applied to a large utility distribution feeder to assess its practical applicability and scalability.

The remainder of this paper is organized as follows. In Section II, we summarize the network model and Kron reduction. Section III formulates a mixed-integer nonlinear programming (MINLP) for optimal Kron-based network reduction. Reformulation to MILP and the first stage reduction are presented in Section IV. We introduce the concept of radialization in section V. Experimental results are presented in Section VI. Finally, the paper concludes in Section VII with a summary and a brief discussion on future directions and applications.

II. NETWORK MODEL AND KRON REDUCTION

A. Network Representation

Consider a power system network as a graph $\mathcal{G} = (\mathcal{V}, \mathcal{E})$, where \mathcal{V} and \mathcal{E} represent the set of n electrical buses and m branches, respectively. The network's structure is defined by the adjacency matrix $\Lambda \in \{0, 1\}^{n \times n}$, where $\Lambda_{ij} = 1$ ($\Lambda_{ij} = 0$) indicates the presence (absence) of an edge between nodes i and j . The nodal admittance matrix, $Y \in \mathbb{C}^{n \times n}$, captures the electrical characteristics of the network. Let $V, I \in \mathbb{C}^n$ denote complex nodal voltage and current injection vectors, respectively, which are related via Kirchhoff's Current Law as

$$I = YV. \quad (1)$$

B. Kron Reduction of Electrical Networks

The Kron reduction of a graph results in a smaller graph by eliminating a subset of nodes with no power injection, while preserving the equivalent impedances among the remaining nodes. Consider a network with an admittance matrix Y , where we divide the nodes into a set of nodes to be kept, denoted

as k , and a set of nodes to be removed, denoted as r . If the current injection at the nodes in set r is zero (i.e., $I_r = 0$), we can partition (1) as:

$$\begin{bmatrix} I_k \\ 0 \end{bmatrix} = \begin{bmatrix} Y_{kk} & Y_{kr} \\ Y_{rk} & Y_{rr} \end{bmatrix} \begin{bmatrix} V_k \\ V_r \end{bmatrix}. \quad (2)$$

The Kron reduction of Y is the Schur complement of Y_{rr} [6]. Thus, the Kron-reduced admittance matrix, denoted as Y_{Kron} , is given by

$$Y_{\text{Kron}} = Y_{kk} - Y_{kr}Y_{rr}^{-1}Y_{rk}, \quad (3)$$

such that

$$I_k = Y_{\text{Kron}}V_k. \quad (4)$$

C. Kron-based Network Reduction

While traditional Kron reductions require reducing on a set of zero-injection nodes, this manuscript allows any set of nodes to be Kron-reduced, which results in a network approximation. Specifically, we are interested in optimally selecting a subset of nodes to be reduced and assigning their injections to nodes that are kept. The aggregation of current injections onto a kept node forms a *super-node*.

To select super-nodes, we define a binary decision matrix, $A \in \{0, 1\}^{n \times n}$, where $A_{i,j} = 1$, if nodal current injection from reduced node j is assigned to kept node i and $A_{i,j} = 0$ otherwise. Specifically, node i is a super-node if $A_{i,i} = 1$ and reduced otherwise.

Since current can only be assigned to one super-node, $\sum_i A_{i,j} = 1$ is always enforced. Furthermore, $\sum_j A_{i,j} \leq A_{i,i}$ ensures that currents cannot be assigned to a reduced bus. Now, we can calculate "Kron currents" as

$$I_{\text{Kron}} = AI, \quad (5)$$

where $I_{\text{Kron}} \in \mathbb{C}^n$ maps the current injections corresponding to reduced nodes to zero. Fig. 2 provides an illustrative example of how super-nodes are formed during the network reduction process. In this study, we assume loads and generations have the same current injections in reduced and full networks. Thus, the nodal voltages of the Kron-based reduced network can be obtained from

$$YV_{\text{agg}} = AI, \quad (6)$$

where $V_{\text{agg}} \in \mathbb{C}^n$ is the voltage of the full network under the aggregated current injections. Since voltages of kept nodes in the full and reduced networks are equal, without using (3)

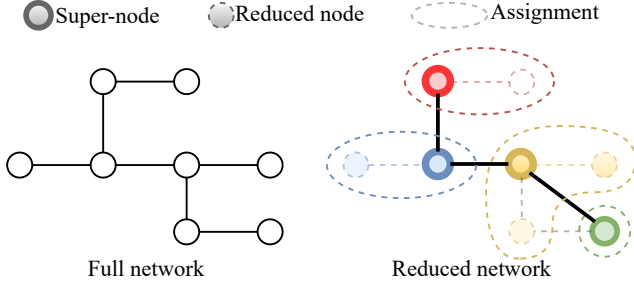


Fig. 2. Opti-KRON procedure; an 8-bus radial network has been reduced to a 4-bus network. The reduced nodes injections are assigned to their super-nodes in each cluster. Reduced network topology and the connections among super-nodes can be found through equation (3).

and (4), we can still compute the super-nodes' voltages resulting from a Kron-based reduction, e.i., (6). Additionally, we would like to represent the voltages at Kron-reduced nodes by those at their respective (kept) super-nodes. This assignment is straightforward using matrix A as

$$V_{\text{Kron}} = A^T V_{\text{agg}}, \quad (7)$$

where $V_{\text{Kron}} \in \mathbb{C}^n$ defines nodal voltages of a Kron-based reduced network. The goal of this manuscript is, therefore, to select nodal assignment matrix A that maximizes the number of reduced *children-nodes*, balanced against how well the selected super-nodes represent their respective children-nodes.

III. OPTIMAL KRON-BASED REDUCTION OF NETWORKS

In this section, we formulate an optimization problem that determines the optimal assignment matrix A , which controls the trade-off between accuracy and reduction by specifying the clusters configuration and the number of super-nodes. Therefore, we need to define an objective function that balances reduction and voltage accuracy.

To quantify accuracy, we define an error metric that measures the deviation between each node's voltage in the full network and the voltage of its super-node in the reduced network. Additionally, to consider different operating conditions we calculate the error with respect to n_L different loading scenarios $l \in \mathcal{L}$. Data for these scenarios comes from representative AC power flow solutions on the full network. We denote the error matrix associated with loading scenario l as

$$E_l = \overbrace{\text{Adiag}\{\hat{V}_l\}}^{\text{Original voltages}} - \overbrace{\text{diag}\{V_l\}A}^{\text{Assigned voltages}} \in \mathbb{C}^{n \times n}, \quad (8)$$

where \hat{V}_l denotes the vector of voltage data in the full network satisfying $Y\hat{V}_l = \hat{I}_l$. Voltage vector V after nodal aggregation is defined by $YV_l = A\hat{I}_l^{-1}$. Based on (8), if $A_{i,j} = 1$, then $E_{l,i,j} = \hat{V}_{l,j} - V_{l,i}$, while $A_{i,j} = 0$ returns $E_{l,i,j} = 0$. To evaluate the worst-case deviation within each cluster, we define the Maximum Intra-Cluster Error (MICE) as

$$\text{MICE}_{l,i} = \|\vec{e}_i^T E_l\|_{\infty}, \quad (9)$$

¹For notational simplicity, we hereafter use V in place of V_{agg} .

where \vec{e}_i represents the i^{th} standard basis vector with all elements zeros except for the i^{th} element. Accordingly, the objective function that optimally balances the trade-off between reduction levels and voltage deviation is then given by:

$$\mathbf{O} = \overbrace{\sum_{l \in \mathcal{L}} \sum_{i \in \mathcal{V}} \|\vec{e}_i^T E_l\|_{\infty}}^{\text{Accuracy}} - \alpha \overbrace{\sum_i^n (1 - A_{i,i})}^{\text{Reduction lev.}}, \quad (10)$$

with α denoting a weighting factor that determines the network reduction priority. The term $\sum_i^n (1 - A_{i,i})$ counts the number of eliminated nodes, as $A_{i,i} = 0$ indicates a reduced node. Given this objective function, we can express the optimization problem as follows:

$$\min_{A, V, E} \sum_{l \in \mathcal{L}} \sum_{i \in \mathcal{V}} \|\vec{e}_i^T E_l\|_{\infty} - \alpha \sum_{i \in \mathcal{V}} (1 - A_{i,i}) \quad (11a)$$

$$\text{s.t.} \quad E_l = A \text{diag}\{\hat{V}_l\} - \text{diag}\{V_l\}A \quad \forall l \in \mathcal{L} \quad (11b)$$

$$YV_l = A\hat{I}_l \quad \forall l \in \mathcal{L} \quad (11c)$$

$$-\bar{E} \leq |A^T V_l| - |\hat{V}_l| \leq \bar{E} \quad \forall l \in \mathcal{L} \quad (11d)$$

$$A^T \mathbf{1} = \mathbf{1} \quad (11e)$$

$$A_{i,j} \leq A_{i,i} \quad \forall i, j \in \mathcal{V} \quad (11f)$$

$$A_{i,j} \leq \Lambda_{i,j} \quad \forall i, j \in \mathcal{V}, i \neq j \quad (11g)$$

$$A_{i,j} \in \{0, 1\} \quad \forall i, j \in \mathcal{V}. \quad (11h)$$

In the proposed model, we can calculate super-nodes voltages for each loading scenario in (11c). Equation (11d) bounds the voltage magnitude deviation to lie within \bar{E} . Here, \bar{E} is the user-defined error limit for voltage magnitude. Each node can only be assigned to one cluster, forced by (11e). According to (11f), reduced nodes can be assigned only to super-nodes. To avoid cases where the optimizer aggregates nodes that are far from each other, we use the adjacency matrix to restrict nodal aggregations to neighboring nodes with (11g). The optimization converges when further reduction violates (11d). Therefore, we should set α to a positive value large enough to incentivize further reduction, but not excessively large that the reduction term dominates the objective. However, (11) represents a non-convex MINLP, and solving it for realistic networks presents computational challenges. Thus, in the following section, we enhance the computational scalability of the network reduction problem.

IV. IMPROVING SCALABILITY

To improve the scalability of (11), we introduce a Kron-based reduction algorithm to selectively reduce a subset of the zero-injection nodes before solving the optimal network reduction problem. In the next step, we reformulate (11) as an MILP. Finally, we add a cutting plane to speed up the MILP.

A. Reduction of Zero-Injection Nodes

At this step, we reduce a subset of zero-injection nodes, defined as $\mathcal{Z} := \{i \in \mathcal{V} \mid \hat{I}_{l,i} = 0, \forall l \in \mathcal{L}\}$. Reduction of these nodes, as shown in (2), does not affect the voltages at the other nodes. For each zero-injection node satisfying the conditions described below, we aim to assign it to a super-node

from the set of non-zero-injection nodes, denoted by $\mathcal{I} := \mathcal{V} \setminus \mathcal{Z}$, and update the assignment matrix A accordingly. These assignments must satisfy the following conditions:

- 1) The voltage magnitude difference between a zero-injection node and its super-node must not exceed the threshold \bar{E} , to satisfy (11d).
- 2) The path between each reduced node and its super-node must contain only zero-injection nodes from the same cluster and no other super-nodes.

However, not all the nodes in \mathcal{Z} will necessarily satisfy these conditions. Algorithm 1 summarizes the procedure to assign eligible zero-injection nodes to super-nodes, where each node $i \in \mathcal{Z}$ is associated with a candidate set $\mathcal{C}_i := \{j \in \mathcal{I} | \pi_{i,j} \subseteq \mathcal{Z}\}$, with $\pi_{i,j}$ representing the set of nodes along the path from node i to node j , excluding node j .

Algorithm 1 Assignment of Zero-Injection Nodes

```

1: Input:  $\Lambda$  (adjacency matrix),  $\hat{V}$  (voltage data),  $\bar{E}$  (voltage
   error bound),  $\mathcal{C}$  (candidate node set),  $\mathcal{Z}$  (zero injection
   node set)
2:  $A \leftarrow I$  ▷ Assign the Identity
3:  $\mathcal{U} \leftarrow \mathcal{Z}$  ▷ Unassigned nodes
4:  $\Delta \leftarrow 1$  ▷ Termination indicator
5:  $d_{i,j} \leftarrow \max_{l \in \mathcal{L}} ||\hat{V}_{l,i}| - |\hat{V}_{l,j}||, \forall i \in \mathcal{Z}, j \in \mathcal{C}_i$ 
6: while  $\Delta = 1$  do
7:    $\Delta \leftarrow 0$ 
8:   for each  $i \in \mathcal{U}$  do
9:     for each  $j \in \mathcal{V} \setminus \mathcal{U}$  such that  $\Lambda_{i,j} = 1$  do
10:       $k \leftarrow \{m \in \mathcal{V} | A_{m,j} = 1\}$ 
11:      if  $d_{i,k} \leq \bar{E}$  and  $d_{i,k} \leq d_{l,i} \forall l \in \mathcal{C}_i$  then
12:         $A_{i,i} \leftarrow 0, A_{k,i} \leftarrow 1$ 
13:         $\mathcal{U} \leftarrow \mathcal{U} \setminus \{i\}, \Delta = 1$ 
14:      end if
15:    end for
16:  end for
17: end while

```

After this process, the proposed optimization problem, finalized later in this section as (23), can be applied to the resulting network to yield an optimal reduced network.

B. Problem Reformulation

To reformulate the non-linear term $\text{diag}\{V_l\}A$ in (11b), we employ the Big M method by defining auxiliary variable $W_l := \text{diag}\{V_l\}A$. This allows us to replace (11b) with its equivalent set of inequality constraints:

$$W_{l,i,j} \leq (1 - A_{i,j})M + V_{l,i} \quad \forall i, j \in \mathcal{V}, \forall l \in \mathcal{L} \quad (12a)$$

$$W_{l,i,j} \geq (A_{i,j} - 1)M + V_{l,i} \quad \forall i, j \in \mathcal{V}, \forall l \in \mathcal{L} \quad (12b)$$

$$W_{l,i,j} \leq MA_{i,j} \quad \forall i, j \in \mathcal{V}, \forall l \in \mathcal{L} \quad (12c)$$

$$W_{l,i,j} \geq -MA_{i,j} \quad \forall i, j \in \mathcal{V}, \forall l \in \mathcal{L} \quad (12d)$$

The parameter M in (12) represents a sufficiently large constant. However, selecting excessively large values can cause numerical challenges during the optimization process [19]. Hence, it is valuable to determine the smallest possible M

that guarantees the feasibility of the constraints without compromising numerical performance. Appendix B discusses the selection of M in more detail. Now, we can update (11b) to

$$E_l = A \text{diag}\{\hat{V}_l\} - W_l \quad \forall l \in \mathcal{L}. \quad (13)$$

To derive a linear approximation of (11d), we first calculate the nodal voltage error as

$$e_l = A^T V_l - \hat{V}_l. \quad (14)$$

We can rewrite (14) as $A^T V_l = \hat{V}_l + e_l$, and update (11d) to

$$|\hat{V}_l| - \bar{E} \leq |\hat{V}_l + e_l| \leq |\hat{V}_l| + \bar{E} \quad \forall l \in \mathcal{L}. \quad (15)$$

In practice, the voltage magnitudes $|\hat{V}_l|$ are typically close to 1 p.u. and $0 \leq \bar{E} \ll 1$, which implies that $|\hat{V}_l| - \bar{E} \geq 0$. Therefore, we can take the square of (15) and simplify it to

$$-2|\hat{V}_l|\bar{E} + \bar{E}^2 - |e_l|^2 \leq 2(\Re\{\hat{V}_l\}\Re\{e_l\} + \Im\{\hat{V}_l\}\Im\{e_l\}) \quad (16a)$$

$$2|\hat{V}_l|\bar{E} + \bar{E}^2 - |e_l|^2 \geq 2(\Re\{\hat{V}_l\}\Re\{e_l\} + \Im\{\hat{V}_l\}\Im\{e_l\}), \quad (16b)$$

where $\Re\{\cdot\}$ and $\Im\{\cdot\}$ denote real and imaginary parts complex values. The upper bound (16a) represents a non-convex constraint. Considering that we are solving the problem in a per-unit system, \bar{E} and e_l represent voltage deviations normalized to the system's base voltage. Accordingly, since $\bar{E}^2 \ll 1$ and $|e_l|^2 \ll 1$, we can approximate (16) with $|e_l|^2 - \bar{E}^2 \approx 0$:

$$-|\hat{V}_l|\bar{E} \leq \Re\{\hat{V}_l\}\Re\{e_l\} + \Im\{\hat{V}_l\}\Im\{e_l\} \quad (17a)$$

$$|\hat{V}_l|\bar{E} \geq \Re\{\hat{V}_l\}\Re\{e_l\} + \Im\{\hat{V}_l\}\Im\{e_l\}. \quad (17b)$$

We consider $\Re\{e_l\}$ and $\Im\{\hat{V}_l\}$ as two distinct variables, as shown in Appendix A. Thus, (17) represents a linear approximation of (11b). In Section VI, we show that the approximation error is negligible for realistic networks.

C. Cutting Plane Restriction

The following cutting plane reduces the feasible set by limiting the number of simultaneous reductions in the network to no more than $q \geq 1$:

$$\sum_{i \in \mathcal{V}} (1 - A_{i,i}) \leq q. \quad (18)$$

Adding (18) to the MILP problem results in a more tractable optimization problem. However, it limits the degree of reduction, which necessitates an iterative approach to reduce networks further. In an iterative approach, the solution at each iteration builds on the optimal solution from the previous iteration. Thus, we need to integrate previous assignments, as determined from A at the optimal point. First, we need to define a new variable $\Omega \in \{0, 1\}^{n \times n}$ that captures only the current iteration's assignments and adjust (11g) as

$$\Omega_{i,j} \leq \Lambda_{i,j} \quad \forall i, j \in \mathcal{V}, i \neq j. \quad (19)$$

Then, the full assignment matrix can be computed from

$$A = \Omega A^{\text{prev}}, \quad (20)$$

where A^{prev} represents optimal A from the previous iteration. For the initial iteration, A^{prev} is derived from the first stage

(Algorithm 1), or, if stage 1 is skipped, it is set to the identity matrix I . To avoid repeatedly considering reduced nodes, we should also update the objective function to

$$\mathbf{O} = \sum_{l \in \mathcal{L}} \sum_{i \in \mathcal{V}} \|\tilde{e}_i^T E_l\|_\infty - \alpha \sum_{i \in \mathcal{V}} (A_{i,i}^{\text{prev}} - A_{i,i}), \quad (21)$$

and (18) as

$$\sum_{i \in \mathcal{V}} (A_{i,i}^{\text{prev}} - A_{i,i}) \leq q. \quad (22)$$

Now, the proposed optimization problem, which we refer to as Opti-KRON, can be stated as:

Opti-KRON

$$\begin{aligned} \min_{\substack{A, V, E \\ \Omega \in \{0,1\}^{n \times n}}} \quad & \sum_{l \in \mathcal{L}} \sum_{i \in \mathcal{V}} \|\tilde{e}_i^T E_l\|_\infty - \alpha \sum_{i=1}^n (A_{i,i}^{\text{prev}} - A_{i,i}) \\ \text{s.t. (11c)} \quad & \text{(Kirchhoff's Current Law)} \\ \text{(11e), (11f), (19), (20)} \quad & \text{(Assignment constraints)} \\ \text{(12), (11b)} \quad & \text{(Error matrix } (E_l) \text{ calculation)} \\ \text{(14), (17)} \quad & \text{(Error bounds)} \\ \text{(22)} \quad & \text{(Cutting plane)} \end{aligned} \quad (23)$$

The formulation in (23) is presented in complex variables. To reformulate using real values only, we apply the rectangular coordinate transformation. Details of the reformulation are presented in Appendix A. Note that (23) represents an MILP with $\text{tr}(A^{\text{prev}}) + \mathbf{1}^T \Lambda \mathbf{1}$ integer decision variables, where at most q node reductions are by (22). Algorithm 2 describes an iterative approach to implement (23).

Algorithm 2 Network Reduction Algorithm

```

1: Input:  $Y, \hat{V}, \hat{I}, \Lambda, A^{\text{prev}}, \alpha, q, \bar{E}$ 
2:  $\Delta \leftarrow \infty$  ▷ Initialize termination indicator
3: while  $\Delta > 0$  do
4:    $A^* \leftarrow$  Solve optimization problem (23)
5:    $\Delta \leftarrow \sum_i (A_{i,i}^{\text{prev}} - A_{i,i}^*)$ 
6:    $\Lambda \leftarrow (A^* \Lambda A^{*\text{T}}) \circ (\mathbf{1}\mathbf{1}^T - I)$ 
7:    $A^{\text{prev}} \leftarrow A^*$ 
8: end while

```

At each iteration, the adjacency matrix Λ is updated to connect each super-node to all neighbors of itself and its assigned child-nodes through $(A^* \Lambda A^{*\text{T}}) \circ (\mathbf{1}\mathbf{1}^T - I)$, where \circ denotes element-wise multiplication. This algorithm continues until no further reduction happens, which implies that any additional reduction would cause the voltage error to exceed \bar{E} . The assignment matrix of the last iteration reveals super-nodes, reduced nodes, and cluster configurations of an optimal Kron-based reduced network. However, the Kron-based formulation will produce a reduced, but meshed, representation of the original network. To recover a radial distribution network, we propose a novel *radialization* procedure next.

V. RADIALIZATION

In this section, we develop a new *radialization* methodology for recovering equivalent radial networks from Kron-reduced

(meshed) networks. Radialization effectively excises all connected, meshed sub-graphs of super-nodes of the reduced network and replaces them by electrically equivalent radial subgraphs. This process is defined next and depends on the following definition and lemma.

Definition 1 (Clique). A subset of nodes $C \subseteq \mathcal{V}$ in a graph $G = (\mathcal{V}, \mathcal{E})$ is called a *clique* if every pair of distinct nodes in C is connected by an edge, i.e., $(i, j) \in \mathcal{E}$ for all $i, j \in C$, $i \neq j$.

Lemma 1. Let $G = (\mathcal{V}, \mathcal{E})$ be a graph representing an electrical network with complex admittance matrix $Y^{\text{full}} \in \mathbb{C}^{n \times n}$. Suppose node $r \in \mathcal{V}$ is Kron-reduced. Then:

- 1) All nodes that were adjacent to r in the original network become directly connected to each other in the reduced network and form a clique.
- 2) The connections among nodes that were not adjacent to r remain unchanged.

Proof. Let $\mathcal{K} \subset \mathcal{V}$ be the set of nodes we keep in the reduced network. We further partition \mathcal{K} into two disjoint subsets: $\mathcal{K}_a = \{i \in \mathcal{K} \mid i \text{ is adjacent to } r\}$ and $\mathcal{K}_f = \{i \in \mathcal{K} \mid i \text{ is not adjacent to } r\}$, where “f” signifies “far”. Without loss of generality, we can partition the admittance matrix as

$$Y^{\text{full}} = \begin{bmatrix} Y_{\mathcal{K}_f, \mathcal{K}_f} & Y_{\mathcal{K}_f, \mathcal{K}_a} & \mathbf{0} \\ Y_{\mathcal{K}_a, \mathcal{K}_f} & Y_{\mathcal{K}_a, \mathcal{K}_a} & Y_{\mathcal{K}_a, r} \\ \mathbf{0} & Y_{r, \mathcal{K}_a} & Y_{rr} \end{bmatrix}, \quad (24)$$

where the zero blocks reflect that no node in \mathcal{K}_f is adjacent to r . Here, Y_{rr} is a scalar, and $Y_{\mathcal{K}_a, r}$ and Y_{r, \mathcal{K}_a} are column and row vectors with no zero entries. Now, considering (3), the Kron reduction of Y^{full} with respect to r can be stated as

$$Y^{\text{Kron}} = \begin{bmatrix} Y_{\mathcal{K}_f, \mathcal{K}_f} & Y_{\mathcal{K}_f, \mathcal{K}_a} \\ Y_{\mathcal{K}_a, \mathcal{K}_f} & Y_{\mathcal{K}_a, \mathcal{K}_a} \end{bmatrix} - \frac{\begin{bmatrix} \mathbf{0} \\ Y_{\mathcal{K}_a, r} \end{bmatrix} \begin{bmatrix} \mathbf{0} & Y_{r, \mathcal{K}_a} \end{bmatrix}}{Y_{rr}}. \quad (25)$$

This simplifies to

$$Y^{\text{Kron}} = \begin{bmatrix} Y_{\mathcal{K}_f, \mathcal{K}_f} & Y_{\mathcal{K}_f, \mathcal{K}_a} \\ Y_{\mathcal{K}_a, \mathcal{K}_f} & Y_{\mathcal{K}_a, \mathcal{K}_a} - \frac{Y_{\mathcal{K}_a, r} Y_{r, \mathcal{K}_a}}{Y_{rr}} \end{bmatrix}. \quad (26)$$

Note that only the lower-right block of (26), which represents the connection among adjacent nodes, changes. Thus, Kron reduction does not affect connectivity between nodes which are non-adjacent to the reduced node. Additionally, the term $Y_{\mathcal{K}_a, r} Y_{r, \mathcal{K}_a}$ is the outer product of two vectors and is, therefore, a fully dense $\text{degree}(r) \times \text{degree}(r)$ matrix. This implies that any two nodes previously adjacent to node r , become directly connected in the reduced network. Thus, the Kron-reduction results in a *clique* of degree r among all adjacent nodes of a reduced node, regardless of the initial graph's topology (e.g., meshed or radial). \square

Lemma 1 exploits the fact that $Y_{\mathcal{K}_f, \mathcal{K}_f}$ is unaffected by the Kron reduction, as first observed in [20], and it addresses Kron reduction of a single node. However, since simultaneous Kron reduction of m nodes is equivalent to m sequential single-node reductions [6], the lemma generalizes to reductions of multiple

nodes. To further elucidate the structure of Kron-reduced radial networks, we recall the definition of maximal cliques:

Definition 2 (Maximal Clique). A clique is *maximal* if it is not included in any larger clique.

When the original network is radial, the cliques introduced by Kron reduction are both maximal and edge-disjoint (i.e., they do not share edges) [21]. Maximal cliques with two nodes form simple edges, while those with three or more introduce cycles (i.e., local meshing). Consequently, a radial network may become a dense network after Kron reduction, e.g., see Fig. 3(b). This motivates the question: *Can we reverse the Kron-based transformation and recover a radial representation?* To address this, we replace each maximal clique of three or more nodes by a radial sub-network. Because the maximal cliques are edge-disjoint, these replacements can be performed independently. Replacing all such maximal cliques yields a fully *radialized* reduced network.

Reference [21] leverages the characteristics of the admittance matrix of each maximal clique as a sub-network to recover a less reduced network, which also exhibits radial topology. This approach involves introducing additional hidden nodes to each maximal clique and determining the radial connections in the reduced network. However, the objective in [21] is to reconstruct the full network from a Kron-reduced network in the absence of the full network's admittance matrix. In contrast, this paper focuses on identifying the *critical* reduced nodes that must be reinserted to the set of super-nodes to recover radiality. Specifically, we demonstrate how to ensure that each maximal clique with three or more nodes can be transformed into a radial sub-graph by reintroducing the minimal subset of previously reduced nodes.

To accomplish this, let $\mathcal{G} := (\mathcal{V}, \mathcal{E})$ again be the full graph representing a radial electrical network, and let $\mathcal{G}_R := (\mathcal{V}_R, \mathcal{E}_R)$ denote its Kron-reduced graph. Consider one of the maximal clique in \mathcal{G}_R , and let $\mathcal{V}_{\text{clique}} \subseteq \mathcal{V}_R \subset \mathcal{V}$ be the set of its nodes with $|\mathcal{V}_{\text{clique}}| \geq 3$. We define $\mathcal{T} = (\mathcal{V}_T, \mathcal{E}_T)$ as the sub-tree of \mathcal{G} that spans all nodes in $\mathcal{V}_{\text{clique}}$, which includes additional nodes from \mathcal{V} to maintain connectivity, such that $\mathcal{V}_{\text{clique}} \subset \mathcal{V}_T$. Since \mathcal{G} is radial, \mathcal{T} is unique [22].

Theorem 1. The nodes in \mathcal{T} with degree ≥ 3 are the minimal subset of previously reduced nodes that must be kept to ensure radial connectivity among the nodes in $\mathcal{V}_{\text{clique}}$.

Proof. To prove Theorem 1, we first show that not reducing the nodes in \mathcal{T} ensures nodes in $\mathcal{V}_{\text{clique}}$ become radially connected. We then show that only nodes of degree ≥ 3 in \mathcal{T} are critical to preserve the radial structure.

Consider the Kron-reduced graph $\tilde{\mathcal{G}}_R = (\tilde{\mathcal{V}}_R, \tilde{\mathcal{E}}_R)$ by replacing the clique on $\mathcal{V}_{\text{clique}}$ in \mathcal{G}_R with the tree \mathcal{T} . Since \mathcal{T} is connected and radial, and none of the nodes in \mathcal{V}_T were reduced, the connections among nodes in \mathcal{T} remain unchanged in $\tilde{\mathcal{G}}_R$. This follows from Lemma 1, which shows that Kron reduction only modifies the connectivity among nodes that are simultaneously adjacent to a reduced node. Thus, in $\tilde{\mathcal{G}}_R$, the paths between nodes in $\mathcal{V}_{\text{clique}}$ lie entirely within \mathcal{T} and remain radial. Moreover, by Lemma 1, any vertex in $\mathcal{V}_T \setminus \mathcal{V}_{\text{clique}}$ with degree at most 2 can still be Kron-reduced from $\tilde{\mathcal{G}}_R$ while

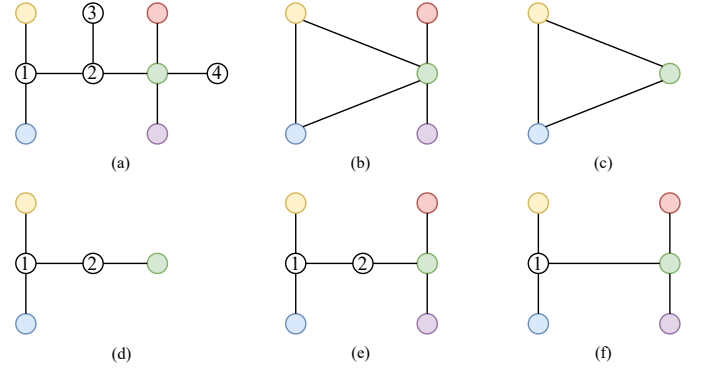


Fig. 3. From a radial network toward a reduced radial network. (a) represents a full network \mathcal{G} . (b) shows the reduced network \mathcal{G}_R . A maximal clique is demonstrated in (c). The spanning sub-tree of the clique \mathcal{T} is represented in (d). (e) shows the augmented Kron-reduced graph $\tilde{\mathcal{G}}_R$. (f) demonstrates the reduced radialized graph. Although node 2 has a degree of 3 in \mathcal{G} , its degree is 2 in \mathcal{T} , and thus it is not a critical node for radiality.

preserving radiality. Consequently, only the vertices of degree ≥ 3 in \mathcal{T} are necessary to preserve radiality among the nodes in the original clique. \square

We can use Theorem 1 to find a reduced, yet radial, network from a meshed Kron reduced network by iteratively identifying nodes that are critical for radialization of each maximal clique. For example, consider the reduced network in Fig. 3 (d) as a maximal clique. Its spanning sub-tree in the full network is represented in Fig. 3 (d), where node 2 is the only node with degree ≥ 3 within the sub-tree. Therefore, Fig. 3 (f) is the radialized network of (d). In this process, the nodal injections of critical nodes are not reassigned. Thus, super-nodes in the radialized networks have the same voltage profile as in the pre-radialized networks and are equivalent. Also, radialization does not affect the errors of Kron-based network reduction.

VI. NUMERICAL CASE STUDIES

This section presents the simulation results for the proposed model applied to the 533-bus distribution test system [23] and a real single phase distribution feeder with 3499 nodes, i.e. South Alburgh test case. The optimization problems in this study were implemented in Julia with JuMP [24] and solved using Gurobi Optimizer 12.0, with the optimality gap set to 0.1%. To evaluate reduction quality, we compare voltage magnitudes resulting from power flow on the reduced networks with those from the full networks. We also compare our method with two nodal clustering algorithms that have been used in the power systems literature on network reductions.

A. 533-Bus Distribution Feeder

This network is a single-line equivalent feeder of a 3-phase system. To simulate the varying operational conditions of the network, we incorporated 2 loading scenarios. Fig. 4 represents the voltage profile for these scenarios. We applied the proposed model to this network and could find different reduction levels. The optimization parameter has been set to $\alpha = 10/n$, and $q = 1$. The effect of changing the voltage magnitude limit, \bar{E} ,

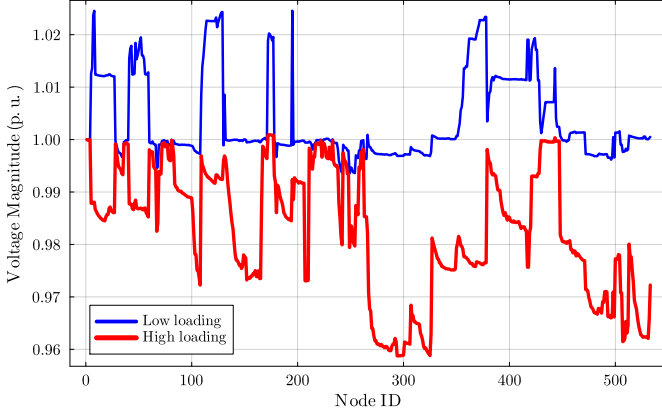


Fig. 4. Voltage profile across 533-bus radial network. Low loading represents the net load of -5 MW and high loading represents the net load of 45 MW.

TABLE I
COMPARISON OF HIGH AND LOW LOADING VOLTAGE ERRORS FOR DIFFERENT REDUCTION LEVELS.

\bar{E} (mp.u.)	Red. (%)	Max (mp.u.)		Mean (mp.u.)		Median (mp.u.)	
		LL	HL	LL	HL	LL	HL
1.0	69	1.0	1.0	0.1	0.3	0.0	0.2
2.5	85	2.4	2.5	0.3	0.7	0.1	0.5
5.0	92	3.5	4.8	0.5	1.5	0.3	1.2
7.5	96	7.2	7.4	1.8	2.6	0.7	2.3
10	97	9.6	9.8	1.4	2.5	0.5	1.9

TABLE II
RADIALIZATION RESULTS FOR THE 533-BUS NETWORK

Initial reduction	Maximal cliques	Critical nodes	Final reduction
69%	13	17	66%
85%	8	15	83%
92%	4	9	90%
96%	2	6	95%
97%	2	4	96%

is summarized in Table I, where LL and HL denote low and high loading conditions, respectively.

As shown in Table I, applying the Opti-KRON formulation reduces the 533-bus distribution feeder by up to 97% with acceptable maximum voltage magnitude errors (i.e., 0.001p.u. or 10mp.u.). However, these reduced networks are not necessarily radial. Therefore, we apply our radialization approach to transform the Kron-reduced networks into radial ones. Table II summarizes how many maximal cliques are present in each reduced network from Table I and shows the number of critical nodes that must be retained to restore a radial topology.

As shown in Table II, increased reduction levels yield fewer maximal cliques. Consequently, the number of critical nodes needed for radialization decreases. Overall, the cost of preserving radial topology—i.e., losing a small fraction in reduction—is relatively small. The full graph of the network is demonstrated in Fig. 5, while super-nodes for the case of 85% reduced network and their clusters have the same colors.

To compare the accuracy and effectiveness of the reduced network on problems beyond basic power flow, we develop an

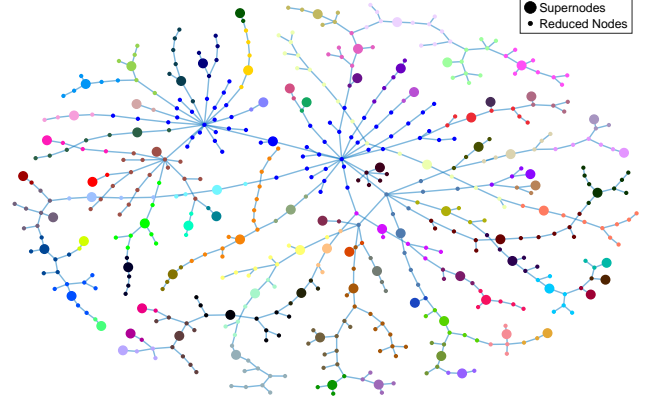


Fig. 5. Graph visualization of the 533-bus full network. Super-nodes and their clusters are shown for 85% reduced network. Nodes with the same color belong to the same cluster.

TABLE III
COMPUTATION TIME AND VOLTAGE ERROR FOR INVERTER DISPATCH OPTIMIZATION PROBLEM WITH DIFFERENT REDUCTION LEVELS.

Reduction	Time (s)		Voltage Error (mp.u.)	
	Meshed	Radialized	Maximum	Mean
0%(Full)	-	18.40	0.00	0.00
69%	10.09	8.46	2.87	0.04
85%	6.11	4.88	3.47	0.14
92%	4.30	3.40	3.54	0.17
96%	2.89	2.59	15.92	0.55
97%	2.71	2.49	18.62	0.62

optimization model to determine the reactive power setpoints for inverters located at distributed generation (DG) buses. The objective of this problem is to minimize the deviation of bus voltages from the nominal 1 p.u. value. The detailed mathematical formulation of this problem is presented in Appendix C. We applied this optimization to both the original and reduced versions of the 533-bus network under 100 loading scenarios. To generate synthetic load scenarios, we applied Singular Value Decomposition (SVD) [25] to historical load data from South Alburgh, Vermont, and fitted a Gaussian Mixture Model (GMM) [26] to model spatial and temporal correlations. We then generated scenarios by sampling from the GMM model and scaled them to match the load limits of the 533-bus system. The voltage solution from the full network was used as the ground truth. After solving the optimization on the reduced network, the obtained reactive power setpoints were applied to a full network power flow, and the resulting voltages were compared to the ground truth. The maximum and mean voltage magnitude errors across all buses and scenarios are reported in Table III.

Table III demonstrates that the proposed network reduction method significantly decreases computational time. While the radialized networks have more nodes, they introduce sparsity in the optimization problem, which speeds up solve times. Even for a 92% reduction, the worst case voltage error remains below 0.004 p.u. (i.e., 4 mp.u.) and the resulting OPF problem was solved up to 5.4 times faster.

TABLE IV
STAGE ② REDUCTION RESULTS ON THE SOUTH ALBURGH FEEDER
COMPARED WITH STAGE ① AND FULL NETWORKS.

\bar{E} (mp.u.)	Max Abs. Error (mp.u.) ① vs. ②	Full vs. ②	Reduction	Opti-KRON Solve time (s)
1.0	0.99	1.8	91%	416.5
2.5	2.49	3.1	93%	481.6
5.0	4.99	5.4	97%	509.9
7.5	7.78	7.8	98%	531.5
10	10.06	10.7	99%	618.6

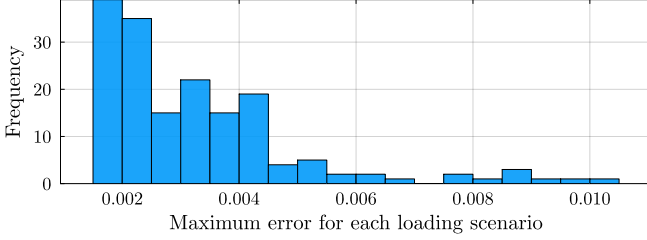


Fig. 6. Histogram of maximum voltage errors across 168 load scenarios on the 94% reduced South Alburgh feeder. Among the 168 scenarios, only 19 exhibit a maximum voltage error ≥ 0.005 p.u., each involving some combination of just 19 distinct nodes out of 3499.

B. 3499-bus South Alburgh feeder

The 3499-bus South Alburgh feeder is a realistic utility distribution system from Vermont. From a week-long dataset of hourly load profiles with 168 scenarios, we selected three representative scenarios corresponding to low, medium, and high loading conditions for the reduction process. We first applied the first stage reduction to reduce zero-injection nodes, using a voltage error threshold of $\bar{E} = 0.001$. We then applied radialization to increase network sparsity for the next stage. This resulted in an initial reduced network with 759 nodes, or a 78% reduction, and an average voltage error of only 0.0002 p.u. In the second stage, we applied Opti-KRON to the initial reduced network. The optimization parameter has been set to $\alpha = 20/n$, and $q = 1$. Finally, we radialized the reduced networks. Table IV represents the reduction result for this network, where “① vs. ②” denotes the maximum absolute error relative to the Stage 1 reduced network, whereas “Full vs. ②” denotes the error relative to the full network. Since \bar{E} restricts the voltage error of final reduced networks with respect to the initial reduced network from the first stage, maximum errors are slightly above \bar{E} . Additionally, the aggregated solve time is summarized in Table IV, which corresponds to the total time Gurobi spent solving the MILP across all iterations of algorithm 2. The average solve time per iteration for this network is approximately 0.75 seconds, which demonstrates that the proposed formulation remains computationally tractable for large-scale networks. To evaluate the robustness of the reduced network obtained using the three representative scenarios, we tested its performance across all 168 loading conditions from the original dataset. We applied a power flow on the 94% reduced network for all the scenarios. Fig. 6 shows the distribution of maximum voltage errors for this power flow problem. Figure 6 demonstrates that in over

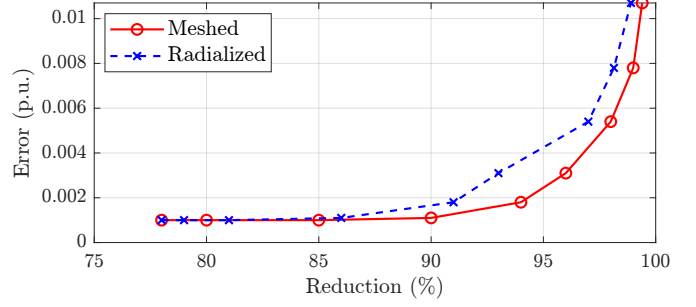


Fig. 7. Maximum voltage magnitude error versus network reduction level for the South Alburgh feeder. The errors shown are from power flow solutions on the full and reduced networks.

TABLE V
VOLTAGE ERROR (IN mp.u.) FOR DIFFERENT REDUCTION METHODS.

Reduction	Opti-KRON		ANAC		ED	
	Max	Mean	Max	Mean	Max	Mean
80%	1.0	0.06	39	0.15	22	0.97
90%	1.1	0.10	39	0.46	23	0.97
95%	3.1	0.40	82	0.85	23	0.96

89% of the scenarios, the maximum voltage error remains below 0.005 p.u. Across all scenarios, only 19 nodes exceed this threshold. Moreover, no scenario includes more than 2 such nodes among the 3499 buses.

To better visualize the trade-off between network reduction and accuracy, Fig. 7 presents the Pareto front obtained from the reduction results for South Alburgh feeder. The results show that both meshed and radialized reductions achieve substantial reductions even under tight voltage error limits, with meshed reductions about 2–3% higher reduction levels.

We tested the inverter dispatch optimal power flow problem (from Appendix C) to the South Alburgh feeder using 168 loading scenarios based on hourly load profiles over a week. Figure 8 shows the maximum and mean voltage magnitude errors, along with OPF solve times, across different reduction levels. The solve times for pre-radialized reduced networks are not strictly decreasing with higher reductions. The reason is that smaller networks may still be more computationally intensive if they are more densely connected. However, this trend is not observed for radialized networks, where the solve time monotonically decreases with higher reductions.

To benchmark the proposed reduction method, we compare it with several clustering-based approaches. In each case, nodes are clustered based on a chosen metric, and the centroid of each cluster is selected as the representative super-node. The reduced network is then formed by applying Kron reduction to reduce non-super-nodes and aggregating all injections in each cluster to its super-node. The first approach is Adjacent Node Agglomerative Clustering (ANAC), introduced in [27]. It restricts clusters to adjacent nodes and finds clusters based on voltage magnitude similarity. The second approach applies clustering on Electrical Distances (ED) [28]. Table V summarizes the nodal voltage deviation in mp.u. obtained with each reduction method on the South Alburgh network. Both ANAC and ED produced significantly higher voltage deviations than

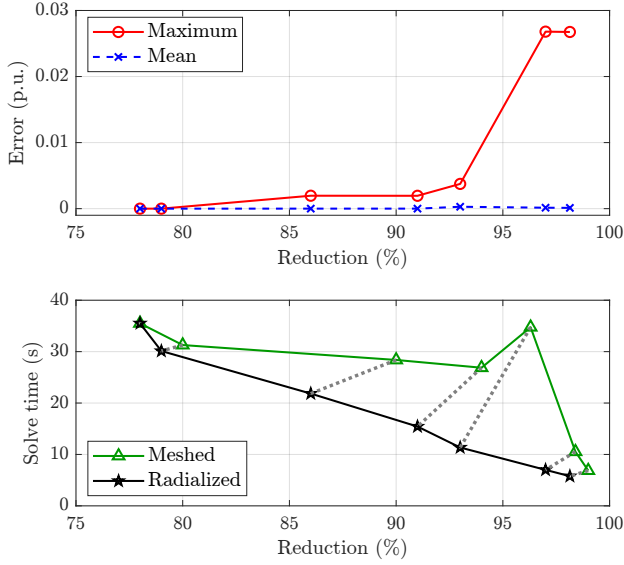


Fig. 8. Voltage magnitude error and solver time for the inverter dispatch optimization problem on the reduced South Alburgh feeder under 168 loading scenarios. The voltage error plot reflects reduction levels based on the radialized networks. The 94% reduced radialized network achieves a 14x speed-up (vs. 157.4 s for the full network) with maximum error below 0.002 p.u. While maximum error increases at high reduction levels, the mean error stays near zero, which indicates that the deviation for most nodes is negligible.

Opti-KRON across all reduction levels. Additionally, the proposed first stage network reduction yields 78% reduction with maximum error less than 0.001 p.u.. This significantly outperforms both ED and ANAC, and demonstrates the effectiveness of the first stage process.

VII. CONCLUSION

This paper introduces a two-stage Kron-based network reduction approach that can be applied to distribution networks. The proposed model performs reliably across diverse loading conditions and demonstrates robustness without significant voltage profile deviations. Testing on a 533-bus radial distribution network achieved an 85% reduction and maintained voltage errors within acceptable limits. Similarly, the proposed two-stage reduction applied to a realistic 3499-bus Vermont feeder significantly reduced network size and ensured acceptable voltage accuracy. Additionally, we introduced a radialization step that recovers a radial structure after Kron reduction. Our results showed that it preserves network structure and improves computational speed.

Future work will expand Opti-KRON to 3-phase (unbalanced) distribution feeders for practical implementations. In particular, we are interested in studying how OPF solutions, DER controller design, and hosting capacity based on the reduced networks can be lifted to the full network and the associated optimality and feasibility gaps that result from such approaches. If the gaps are practical, the Opti-KRON could serve to potentially scale up distribution grid computations significantly across different domains. Lastly, we are interested in understanding how we can adapt Opti-KRON concepts for network reduction problems related to Markov decision processes, neural networks, and other networks.

APPENDIX

A. Rectangular Reformulation of the Optimization Problem

While the Opti-KRON formulation in (23) is expressed using complex variables, it is reformulated in real rectangular coordinates so that standard optimization solvers can solve it. To do so, we first substitute (11c) by the following equations:

$$\Re(\mathbf{Y})V_l^{\text{Re}} - \Im(\mathbf{Y})V_l^{\text{Im}} = A\Re(\hat{I}) \quad \forall l \in \mathcal{L} \quad (27)$$

$$\Re(\mathbf{Y})V_l^{\text{Im}} + \Im(\mathbf{Y})V_l^{\text{Re}} = A\Im(\hat{I}) \quad \forall l \in \mathcal{L}, \quad (28)$$

where V_l^{Re} and V_l^{Im} are real and imaginary parts of V_l . Accordingly, we adjust (12) for $\forall i, j \in \mathcal{V}$ and $\forall l \in \mathcal{L}$ as

$$W_{l,i,j}^{\text{Re}} \leq (1 - A_{i,j})M_{l,i}^{\text{Re}} + V_{l,i}^{\text{Re}} \quad (29a)$$

$$W_{l,i,j}^{\text{Re}} \geq (A_{i,j} - 1)M_{l,i}^{\text{Re}} + V_{l,i}^{\text{Re}} \quad (29b)$$

$$W_{l,i,j}^{\text{Re}} \leq M_{l,i}^{\text{Re}} A_{i,j} \quad (29c)$$

$$W_{l,i,j}^{\text{Re}} \geq -M_{l,i}^{\text{Re}} A_{i,j}. \quad (29d)$$

W^{Im} is similarly defined. Similarly, (13) is decomposed to

$$E_l^{\text{Re}} = A \text{diag}\{\Re\{\hat{V}_l\}\} - W_l^{\text{Re}} \quad (30a)$$

$$E_l^{\text{Im}} = A \text{diag}\{\Im\{\hat{V}_l\}\} - W_l^{\text{Im}}. \quad (30b)$$

E_l^{Re} and E_l^{Im} represent real and imaginary parts of the error matrix. Additionally, (14) transforms into

$$e_l^{\text{Re}} = \Re\{\hat{V}_l\} - A^T V_l^{\text{Re}} \quad (31a)$$

$$e_l^{\text{Im}} = \Im\{\hat{V}_l\} - A^T V_l^{\text{Im}}. \quad (31b)$$

However, (17) is already decomposed into rectangular form. Thus, Opti-KRON can be stated as:

$$\begin{aligned} \min_{\mathbb{E}} \quad & \sum_{l \in \mathcal{L}} \sum_{i \in \mathcal{V}} (\|\tilde{e}_i^T E_l^{\text{Re}}\|_{\infty} + \|\tilde{e}_i^T E_l^{\text{Im}}\|_{\infty}) \\ & - \alpha \sum_{i \in \mathcal{V}} (A_{i,i}^{\text{prev}} - A_{i,i}) \end{aligned} \quad (32a)$$

$$(11e), (11f), (11h) - (20), (17), (22), (27) - (31), \quad (32b)$$

where $\mathbb{E} = \{A, \Omega, V^{\text{Re}}, V^{\text{Im}}, E^{\text{Re}}, E^{\text{Im}}, e^{\text{Re}}, e^{\text{Im}}, W^{\text{Re}}, W^{\text{Im}}\}$.

B. Bounds on Big M

In this subsection, we derive tight yet feasible bounds on the Big M constants in (29) to reduce solve time of (32). At each iteration k , we propose setting the Big M constants to

$$M_{l,i}^{\text{Re}}(k) := \text{MICE}_{l,i}^{k-1} + \alpha q + \Re(\hat{V}_{l,i}), \quad (33a)$$

$$M_{l,i}^{\text{Im}}(k) := \text{MICE}_{l,i}^{k-1} + \alpha q + \Im(\hat{V}_{l,i}), \quad (33b)$$

where $\text{MICE}_{l,i}^{k-1} := \|\tilde{e}_i^T E_l^{\text{Re}}\|_{\infty} + \|\tilde{e}_i^T E_l^{\text{Im}}\|_{\infty}$ is computed using the optimal solution from iteration $k-1$. E_l^{Re} and E_l^{Im} are introduced in (30). We now prove that the proposed bound for $M_{l,i}^{\text{Re}}$ is feasible and tight relative to the value of MICE. To preserve feasibility of (29), we require $M_{l,i}^{\text{Re}} \geq V_{l,i}^{\text{Re}} = \Re(\hat{V}_{l,i}) + e_{l,i}^{\text{Re}}$. Accordingly, we need to find an upper bound on $e_{l,i}^{\text{Re}}$ to obtain a feasible value for $M_{l,i}^{\text{Re}}$. We can rewrite the objective function at iteration k as

$$O^k = \sum_{l \in \mathcal{L}} \sum_{i \in \mathcal{V}} \text{MICE}_{l,i}^k - \alpha \sum_i (A_{i,i}^{\text{prev}} - A_{i,i}^k). \quad (34)$$

The term $-\alpha \sum_i (A_{i,i}^{\text{prev.}} - A_{i,i}^k)$ incentivizes further node reduction: it decreases the objective by α for each node reduced in iteration k and is zero otherwise. When this decrease outweighs the change in the first term between iterations $k-1$ and k , more nodes are reduced. Accordingly,

$$\alpha \sum_{i \in \mathcal{V}} (A_{i,i}^{\text{prev.}} - A_{i,i}^k) \geq \sum_{l \in \mathcal{L}} \sum_{i \in \mathcal{V}} (\text{MICE}_{l,i}^k - \text{MICE}_{l,i}^{k-1}). \quad (35)$$

$$\geq \text{MICE}_{l,i}^k - \text{MICE}_{l,i}^{k-1}. \quad (36)$$

The cutting-plane constraint (22) limits the number of nodes that can be reduced in any iteration to at most q . Therefore,

$$\alpha q \geq \text{MICE}_{l,i}^k - \text{MICE}_{l,i}^{k-1}, \quad (37)$$

which yields

$$\alpha q + \text{MICE}_{l,i}^{k-1} \geq \|\bar{e}_i^T E_l^{\text{Re}}\|_{\infty} + \|\bar{e}_i^T E_l^{\text{Im}}\|_{\infty}. \quad (38)$$

Since $e_{l,i}^{\text{Re}} \leq \|\bar{e}_i^T E_l^{\text{Re}}\|_{\infty}$, we have $\alpha q + \text{MICE}_{l,i}^{k-1} \geq e_{l,i}^{\text{Re}}$, which provides an upper bound on $e_{l,i}^{\text{Re}}$. The derivation for $M_{l,i}^{\text{Im}k}$ follows analogously. Thus, the Big M constants in (33a) and (33b) are guaranteed to be feasible.

C. Reactive Power Adjustment Optimization Problem

This appendix presents the mathematical formulation of the reactive power optimization problem used to validate the reduced networks. The objective is to adjust inverter reactive power setpoints to minimize voltage magnitude deviations with AC power flow and operational constraints.

$$\min_{|V|, \theta, q^{\text{inv}}, p^g, q^g} \sum_{i \in \mathcal{N}} ||V_i| - 1| \quad (39a)$$

$$\text{s.t. } P_i + p_{i|i=\text{slack}}^g = \sum_{k \in \mathcal{N}} |V_i| |V_k| G_{i,k} \cos(\theta_i - \theta_k) + |V_i| |V_k| B_{i,k} \sin(\theta_i - \theta_k) \quad \forall i \quad (39b)$$

$$Q_i + q_{i|i=\text{slack}}^g + q_i^{\text{inv}} = \sum_{k \in \mathcal{N}} |V_i| |V_k| G_{i,k} \sin(\theta_i - \theta_k) - |V_i| |V_k| B_{i,k} \cos(\theta_i - \theta_k) \quad \forall i \quad (39c)$$

$$(q_i^{\text{inv}})^2 \leq S_{\max,i}^2 - (p_i^{\text{inv}})^2 \quad \forall i \in \mathcal{S} \quad (39d)$$

$$V_{\min} \leq |V_i| \leq V_{\max} \quad \forall i. \quad (39e)$$

Equation (39a) defines the objective of minimizing the sum of voltage magnitude deviations from 1 p.u. across all buses. Equations (39b) and (39c) represent the nonlinear AC power flow constraints for real and reactive power, including inverter contributions. Parameters P and Q are the injections of load, while p^g and q^g are variables that represent slack bus active and reactive outputs. Constraint (39d) ensures that each inverter operates within its apparent power limit. Constraints (39e) and enforce voltage magnitude bounds.

REFERENCES

- [1] "Grid modernization strategy 2024," U.S. Department of Energy, Tech. Rep. 2024.
- [2] X. Cheng and T. Overbye, "PTDF-based power system equivalents," *IEEE Transactions on Power Systems*, vol. 20, no. 4, pp. 1868–1876, 2005.
- [3] H. Oh, "Aggregation of buses for a network reduction," *IEEE Transactions on Power Systems*, vol. 27, no. 2, pp. 705–712, 2012.
- [4] D. Shi and D. J. Tylavsky, "A novel bus-aggregation-based structure-preserving power system equivalent," *IEEE Transactions on Power Systems*, vol. 30, no. 4, pp. 1977–1986, 2015.
- [5] J. B. Ward, "Equivalent circuits for power-flow studies," *Electrical Engineering*, vol. 68, no. 9, pp. 794–794, 1949.
- [6] F. Dörfler and F. Bullo, "Kron reduction of graphs with applications to electrical networks," *IEEE Transactions on Circuits and Systems I: Regular Papers*, vol. 60, no. 1, pp. 150–163, 2013.
- [7] Q. Ploussard, L. Olmos, and A. Ramos, "An efficient network reduction method for transmission expansion planning using multicut problem and Kron reduction," *IEEE Transactions on Power Systems*, vol. 33, no. 6, pp. 6120–6130, 2018.
- [8] R. Ribeiro, A. Street, F. Mancilla-David, and A. Angulo, "Equivalent reduced DC network models with nonlinear load functions: A data-driven approach," *IEEE Transactions on Power Systems*, vol. 39, no. 2, pp. 3021–3032, 2024.
- [9] W. Lin, C. Zhao, M. Gao, and C. Y. Chung, "Data-driven static equivalence with physics-informed Koopman operators," *CSEE Journal of Power and Energy Systems*, vol. 10, no. 1, pp. 432–438, 2024.
- [10] B. Taheri and D. K. Molzahn, "AC power flow informed parameter learning for DC power flow network equivalents," in *2024 IEEE Texas Power and Energy Conference (TPEC)*, 2024, pp. 1–6.
- [11] Y. Zhu and D. Tylavsky, "An optimization-based DC-network reduction method," *IEEE Transactions on Power Systems*, vol. 33, no. 3, pp. 2509–2517, 2018.
- [12] M. Doquet, "Zonal reduction of large power systems: Assessment of an optimal grid model accounting for loop flows," *IEEE Transactions on Power Systems*, vol. 30, no. 1, pp. 503–512, 2015.
- [13] Z. K. Pecanak, V. R. Disfani, M. J. Reno, and J. Kleissl, "Inversion reduction method for real and complex distribution feeder models," *IEEE Transactions on Power Systems*, vol. 34, no. 2, pp. 1161–1170, 2019.
- [14] Z. K. Pecanak, V. R. Disfani, M. J. Reno, and J. Kleissl, "Multiphase distribution feeder reduction," *IEEE Transactions on Power Systems*, vol. 33, no. 2, pp. 1320–1328, 2018.
- [15] S. Chevalier and M. R. Almassalkhi, "Towards optimal Kron-based reduction of networks (Opti-KRON) for the electric power grid," in *2022 IEEE 61st Conference on Decision and Control (CDC)*, 2022, pp. 5713–5718.
- [16] M. Baran and F. Wu, "Optimal sizing of capacitors placed on a radial distribution system," *IEEE Transactions on Power Delivery*, vol. 4, no. 1, pp. 735–743, 1989.
- [17] G. W. Chang, S. Y. Chu, and H. L. Wang, "An improved backward/forward sweep load flow algorithm for radial distribution systems," *IEEE Transactions on Power Systems*, vol. 22, no. 2, pp. 882–884, 2007.
- [18] R. Jabr, "Radial distribution load flow using conic programming," *IEEE Transactions on Power Systems*, vol. 21, no. 3, pp. 1458–1459, 2006.
- [19] J. D. Camm, A. S. Raturi, and S. Tsubakitani, "Cutting Big M down to size," *Interfaces*, vol. 20, no. 5, pp. 61–66, 1990.
- [20] G. Cavraro and V. Kekatos, "Graph algorithms for topology identification using power grid probing," *IEEE Control Systems Letters*, vol. 2, no. 4, pp. 689–694, 2018.
- [21] Y. Yuan, S. H. Low, O. Ardakanian, and C. J. Tomlin, "Inverse power flow problem," *IEEE Transactions on Control of Network Systems*, vol. 10, no. 1, pp. 261–273, 2023.
- [22] R. Diestel, *Graph Theory* (Graduate Texts in Mathematics). Springer Berlin Heidelberg, 2018.
- [23] Malmer, Gabriel and Thorin, Lovisa, *Network reconfiguration for renewable generation maximization*, eng. Student Paper, 2023.
- [24] M. Lubin, O. Dowson, J. Dias Garcia, J. Huchette, B. Legat, and J. P. Vielma, "JuMP 1.0: Recent improvements to a modeling language for mathematical optimization," *Mathematical Programming Computation*, 2023.
- [25] R. A. Horn and C. R. Johnson, *Matrix analysis*. Cambridge university press, 2012.
- [26] C. M. Bishop and N. M. Nasrabadi, *Pattern recognition and machine learning*. Springer, 2006, vol. 4.
- [27] B. Stöckl, Y. Werner, and S. Wogrin, *Congestion-sensitive grid aggregation for DC optimal power flow*, 2025. arXiv: 2505.07545.
- [28] M. Almassalkhi, S. Brahma, N. Nazir, et al., "Hierarchical, grid-aware, and economically optimal coordination of distributed energy resources in realistic distribution systems," *Energies*, vol. 13, no. 23, 2020.